Virology **263,** 290–306 (1999)
Article ID viro.1999.9946, available online at http://www.idealibrary.com on IDEAL®

Role of the C-Terminal RDEL Motif of the Myxoma Virus M-T4 Protein in Terms of Apoptosis Regulation and Viral Pathogenesis

Shawna Hnatiuk,* Michele Barry,† Wei Zeng,* Liying Liu,* Alexandra Lucas,* Dean Percy,‡ and Grant McFadden*,[1]

*Department of Microbiology and Immunology, The University of Western Ontario and The John P. Robarts Research Institute, London, Ontario, Canada, N6G 2V4; †Department of Biochemistry, University of Alberta, Edmonton, Canada; and ‡Department of Pathobiology, Ontario Veterinary College, University of Guelph, Guelph, Canada

Received June 12, 1999; returned to author for revision July 7, 1999; accepted August 2, 1999

The purpose of this study was to investigate the significance of the C-terminal RDEL motif of the myxoma virus M-T4 protein in terms of apoptosis regulation and role in viral virulence. To accomplish this, a recombinant myxoma virus was created in which the C-terminal RDEL motif of M-T4 was deleted and a selectable marker (*Eco*gpt) was inserted immediately downstream. We hypothesized that removal of the RDEL motif from M-T4 would alter the subcellular localization of the protein and provide insight into its antiapoptotic role. Surprisingly, removal of the RDEL motif from M-T4 did not affect localization of the protein within the endoplasmic reticulum (ER), but it did reduce the stability of the mutant protein. Pulse-chase immunoprecipitation and endoglycosidase H analysis coupled with confocal fluorescent light microscopy demonstrated that the M-T4 RDEL$^-$ mutant protein is retained in the ER like wildtype M-T4 and suggests that the C-terminal RDEL motif is not the sole determinant for M-T4 localization to the ER. Infection of cultured rabbit lymphocytes with the M-T4 RDEL$^-$ mutant virus results in an intermediate apoptosis phenotype compared with the wildtype and M-T4 knockout mutant viruses. A novel myxomatosis phenotype was observed in European rabbits when infected with the recombinant M-T4 RDEL$^-$ mutant virus. Rabbits infected with the M-T4 RDEL$^-$ virus on day 9 postinfection exhibited an exacerbated edematous and inflammatory response at secondary sites of infections, particularly the ears. Our results indicate that the C-terminal RDEL motif may not be solely responsible for retention of M-T4 to the ER and that M-T4 may have a dual function in protecting infected lymphocytes from apoptosis and in modulating the inflammatory response to virus infection.

INTRODUCTION

To counter the innate and acquired immune defenses devised by vertebrate organisms to combat infections, viruses have responded by developing equally effective anti-immune mechanisms of self-defense (reviewed in McFadden *et al.,* 1995; Ploegh, 1998; Smith, 1994; Spriggs, 1996). Poxviruses in particular contain large double-stranded DNA genomes and encode a large number of anti-immune molecules to subvert the innate and acquired immune responses of the infected host (Nash *et al.,* 1999; Smith *et al.,* 1997).

Infection of the domestic European rabbit (*Oryctolagus cuniculus*) with the poxvirus myxoma virus results in a systemic lethal disease known as myxomatosis (Fenner and Ratcliffe, 1965; Fenner and Ross, 1994; McFadden and Graham, 1994). Based on cellular localization, mode of action, and target, myxoma virus immunomodulatory proteins can be grouped into three major classes: viroceptors, virokines, and viromitigators (Nash *et al.,* 1999). Viroceptors are secreted or membrane-bound virus-encoded cytokine receptor homologs that mimic cellular receptors and thus scavenge extracellular cytokines. For example, myxoma virus encodes a secreted tumor necrosis factor (TNF) receptor (Schreiber and McFadden, 1994; Schreiber *et al.,* 1997), and a secreted interferon (IFN)-γ receptor (Mossman *et al.,* 1996b, 1995; Upton *et al.,* 1992). These viral proteins bind and inhibit TNF and IFN-γ, respectively, thereby inhibiting the antiviral effects of these cytokines. A soluble chemokine binding protein with specificity for CC-chemokines has also been recently described in myxoma virus (Graham *et al.,* 1997; Lalani *et al.,* 1999, 1998). Virokines are virus-encoded versions of secreted cellular cytokines, growth factors, or extracellular immune molecules, and myxoma virus encodes two such examples to date: a secreted serine proteinase inhibitor (Macen *et al.,* 1993; Nash et al., 1997, 1998) and an epidermal growth factor homolog (Opgenorth *et al.,* 1992a,b).

The term "viromitigator" has been coined to refer to intracellular viral proteins that interrupt signal transduction pathways or apoptosis cascades (Nash *et al.,* 1999). Myxoma virus has been shown to encode a variety of proteins that block or delay apoptosis of infected lymphocytes (McFadden and Barry, 1998; Turner and Moyer, 1998). Infection of a recombinant myxoma virus null for M-T5, M-T2, M11L, or M-T4 expression results in apoptosis in a CD4$^+$ rabbit lymphocyte cell line (Barry *et al.,* 1997; Macen *et al.,* 1996; Mossman *et al.,* 1996a). The

[1] To whom reprint requests should be addressed. Fax: (519) 663-3847. E-mail: mcfadden@rri.on.ca.

0042-6822/99 $30.00

myxoma viral protein M-T4 is a novel, endoplasmic reticulum (ER) retained poxviral protein that has a role in both apoptosis inhibition and viral pathogenesis (Barry *et al.,* 1997). The protein has no cellular homologues but contains a putative N-terminal signal sequence and a C-terminal RDEL motif, which has previously been shown to function as an ER retention signal (Pelham, 1989; Pelham, 1990). Studies have determined that M-T4 localizes to the ER of infected cells, and disruption of the gene results in attenuation in European rabbits and the induction of apoptosis in infected $CD4^+$ rabbit T lymphocytes (Barry *et al.,* 1997).

To date, M-T4 is the only known viral ER resident protein shown to have a role in protecting infected cells from apoptosis (McFadden and Barry, 1998). Few clues exist to reveal the mechanism by which M-T4 may exert its antiapoptotic function, but the RDEL motif present at the C-terminus of the M-T4 protein may be crucial to ER localization or for function as a viral apoptosis inhibitor. In this study, we describe the construction of a recombinant myxoma virus in which the C-terminal RDEL motif of the myxoma virus M-T4 gene has been deleted. Mutant M-T4 $RDEL^-$ protein was found to have a shorter half-life than the wildtype M-T4 protein but is surprisingly still localized to the ER. Infection of $CD4^+$ rabbit T lymphocytes with the M-T4 $RDEL^-$ mutant virus results in a semipermissive replicative cycle, corresponding to only a partial inhibition of apoptosis. Furthermore, infection of European rabbits with the M-T4 $RDEL^-$ myxoma virus revealed a novel phenotype associated with increased inflammatory responses at secondary sites of infection. This unexpected association between apoptosis dysregulation and exacerbated inflammation is discussed in terms of M-T4 localization and function.

RESULTS

Construction of an M-T4 $RDEL^-$ mutant virus

Initial sequence analysis of M-T4 revealed a putative N-terminal signal sequence and a C-terminal RDEL motif but no obvious sequence similarity with known cellular proteins (Barry *et al.,* 1997; Upton *et al.,* 1987). A C-terminal RDEL or KDEL motif is generally considered to be a signal for ER retention mediated by the KDEL receptor (Nilsson and Warren, 1994; Pelham, 1989). We postulated that the M-T4 RDEL motif was critical not only for its localization in the ER but also for its function as an antiapoptotic protein during myxoma virus infection. To characterize the role of the C-terminal RDEL motif in M-T4, a recombinant myxoma virus was created in which this motif was removed and replaced with a stop codon followed by a downstream cassette expressing the dominant selectable marker *Escherichia coli* guanosine phosphoribosyl transferase (*Eco* gpt) gene (see Materials and Methods). The RDEL-minus construct (pT7BlueT4$RDEL^-$gpt) contains the 3′ coding region of M-T4 up to, but not including the RDEL motif, the *Eco* gpt cassette and the 5′ region of the flanking open reading frame M-T3. Homologous recombination between this construct and vMyxlac plus selection for gpt expressing virus allowed selection of the recombinant virus vMyxlacT4 $RDEL^-$, in which both copies of the M-T4 gene were replaced with the $RDEL^-$ version. Construction of purified vMyxlacT4 $RDEL^-$ virus was confirmed by PCR analysis with primers that flanked the gpt cassette (data not shown).

M-T4 $RDEL^-$ mutant protein is not secreted

Native M-T4 was predicted to be retained in the ER due to the C-terminal RDEL motif, and thus the removal of the RDEL motif from M-T4 might generate a mutant protein that could exit the ER. Because the KDEL receptor that recycles such proteins back to the ER from the *cis*–Golgi complex can presumably no longer recognize the protein and transport it back to the ER via retrograde transport, we hypothesized that M-T4 $RDEL^-$ would now follow the normal default secretory pathway of the cell. To determine the cellular localization of the M-T4 $RDEL^-$ protein, an antibody to the N-terminal sequence of M-T4 following the predicted signal sequence cleavage site was generated, because the previously described M-T4 C-terminal peptide antibody (made to the last 10 amino acid residues of M-T4) likely would not recognize M-T4 $RDEL^-$ variant protein (Barry *et al.,* 1997). To determine whether M-T4 $RDEL^-$ was in fact secreted, total cellular lysates and secreted proteins were harvested from mock-, vMyxlacT4$^-$-, vMyxlacT4 $RDEL^-$-, vMyxlac-, VV601-, and VVT4-infected baby green monkey kidney (BGMK) cells at 16 h p.i. The lysates and secreted proteins were subjected to Western blot analysis using both the N- and C-terminal M-T4 peptide antibodies. Figure 1A depicts M-T4 as a 30-kDa protein in vMyxlac and VVT4 lysates (lanes 4 and 6) as previously shown (Barry *et al.,* 1997). A slightly smaller protein is detected in vMyxlacT4 $RDEL^-$ lysates in Fig. 1A (lane 3), indicative of M-T4 $RDEL^-$. This band is not observed with the C-terminal M-T4 peptide antibody (data not shown), indicating that the RDEL motif is indeed crucial for this antibody to recognize M-T4, and confirming that the RDEL motif is removed from the M-T4 $RDEL^-$ protein. No comparable protein is detected in mock or vMyxlacT4$^-$ lysates or secreted proteins as expected, but a cross-reacting 35-kDa species was noted in VV-infected cells with the N-terminal M-T4 antibody (Fig. 1A, lanes 5 and 6). The intensity of the M-T4 $RDEL^-$ band detected from vMyxlacT4 $RDEL^-$ infection (Fig. 1A, lane 3) is much less than that observed with wildtype M-T4 from vMyxlac expression in the lysates (Fig. 2A, lane 4), suggesting either lower expression levels or reduced stability of the M-T4 mutant protein. These possibilities are discussed later. Surprisingly, no M-T4 $RDEL^-$ mutant protein was de-

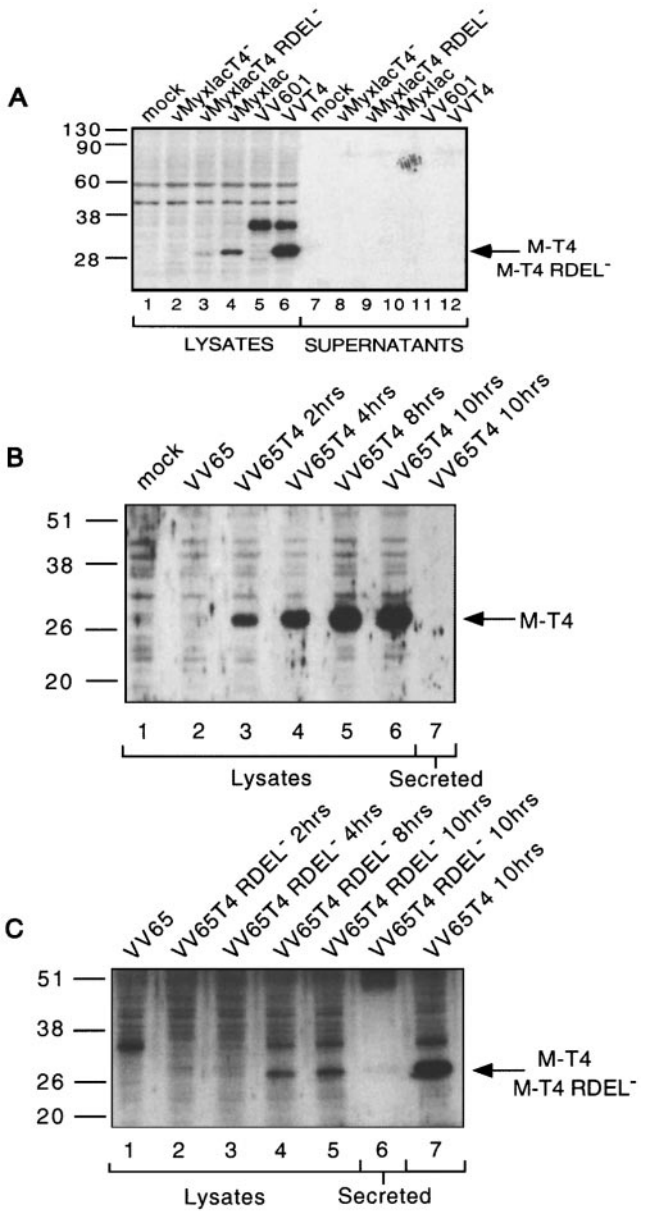

FIG. 1. Expression of the MT4 RDEL$^-$ mutant protein from recombinant myxoma and vaccinia viruses. (A) BGMK cells were mock infected (lanes 1 and 7) or infected with vMxylacT4$^-$ (lanes 2 and 8), vMyxlacT4 RDEL$^-$ (lanes 3 and 9), vMyxlac (lanes 4 and 10), VV601 (lanes 5 and 11), or VVT4 (lanes 6 and 12) at an m.o.i. of 10 PFU/cell for 16 h. VVT4 is a recombinant vaccinia virus that overexpresses the M-T4 cassette, and VV601 is the parental negative control vaccinia virus. Total cell lysates and secreted protein fractions (concentrated fourfold) were harvested and subjected to SDS–PAGE and analyzed by Western blotting with an antibody specific to the N-terminal of M-T4. (B) BGMK cells were mock infected or infected with VV65 or VV65T4 at an m.o.i. of 10 PFU/cell for 16 h. VV65T4 total cell lysates were harvested at 2 h (lane 3), 4 h (lane 4), 8 h (lane 5), and 10 h (lane 6) p.i. Mock (lane 1) and VV65 (lane 2) total cell lysates were harvested at 10 h p.i. VV65T4 secreted protein fractions were also harvested at 10 h p.i. (lane 7). Lysates and secreted protein fractions were subjected to SDS–PAGE and Western blotting analysis with an antibody specific for the C-terminal of M-T4. (C) BGMK cells were infected with VV65, VV65T4 RDEL$^-$, or VV65T4 at an m.o.i. of 10 PFU/cell for 16 h. VV65T4 RDEL$^-$ total cell lysates were harvested at 2 h (lane 2), 4 h (lane 3), 8 h (lane 4), and 10 h (lane 5) p.i.

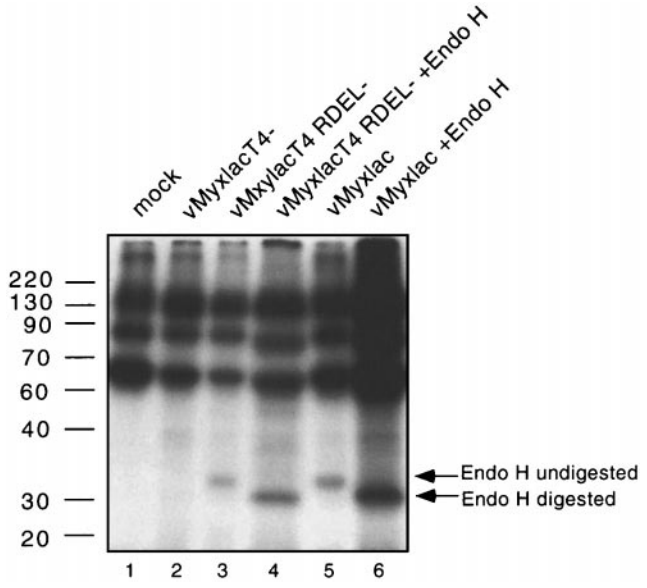

FIG. 2. Immunoprecipitation and endo H analysis of M-T4 and M-T4 RDEL$^-$ from myxoma virus infection. BGMK cells were mock infected (lane 1) or infected with vMyxlacT4$^-$ (lane 2), vMyxlacT4 RDEL$^-$ (lanes 3 and 4), or vMyxlac (lanes 5 and 6). All samples were labeled with ^{35}S Met/Cys at 4–6 h p.i. and immunoprecipitated with antiserum specific to the N-terminal of M-T4. Samples were treated with endo H (lanes 4 and 6) before SDS–PAGE and analysis by autoradiography.

tected in secreted protein fractions of infected cells (Fig. 1A, lane 9). To confirm that the secretory pathway of vMyxlacT4 RDEL$^-$-infected cells is functional, the myxoma virus protein M-T7 was used as a positive control for viral protein secretion because M-T7 synthesis and export during myxoma virus infection have been well characterized (Upton *et al.,* 1992; Mossman *et al.,* 1995). Total cell lysates were harvested as above, and total secreted proteins were concentrated 50-fold to increase detection levels. Western blot analysis with the N-terminal M-T4 peptide antibody still did not reveal any M-T4 RDEL$^-$ protein in the secreted protein fraction (data not shown), even though the 37-kDa M-T7 was detected at comparable levels in the secreted protein fractions of both vMyxlacT4 RDEL$^-$ and vMyxlac, suggesting that the bulk secretory pathway of cells infected with both viruses was unimpaired. At this point, we concluded that M-T4 RDEL$^-$ protein was not secreted but rather was retained within the infected cell, possibly at the cell surface, within the Golgi complex and/or the ER itself.

To maximize detection levels for the RDEL$^-$ variant and wildtype M-T4 proteins, a synthetic vaccinia virus early-late promoter (Chakrabarti *et al.,* 1997) was used to

VV65 (lane 1) and VV65T4 (lane 7) total cell lysates were harvested at 10 h p.i. VV65T4 RDEL$^-$ secreted protein fractions were also harvested at 10 h p.i. (lane 6). Lysates and secreted protein fractions were subjected to SDS–PAGE and Western blotting analysis with an antibody specific for the N-terminal of M-T4.

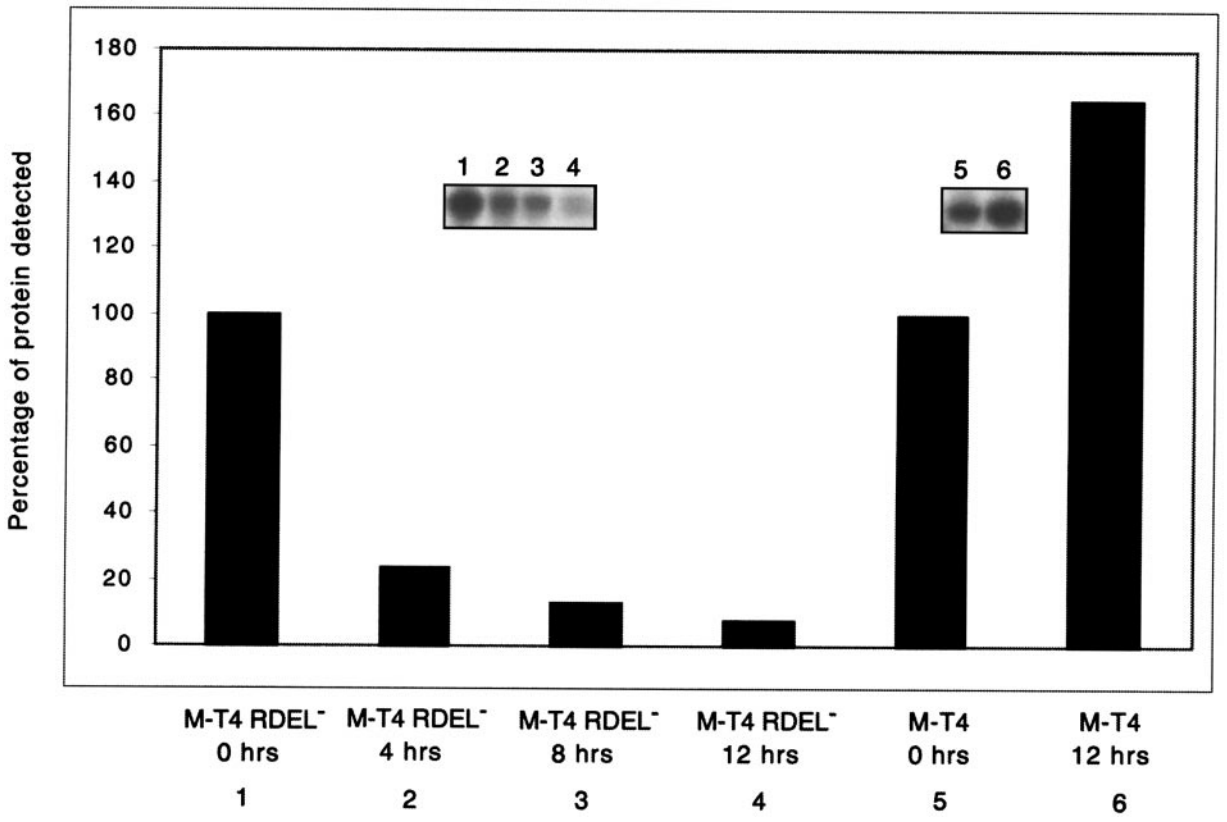

FIG. 3. M-T4 RDEL⁻ and M-T4 protein stability during viral infection. Stability of pulse-labeled M-T4 and M-T4 RDEL⁻ mutant during a 12-h chase period. M-T4 RDEL⁻ and M-T4 were immunoprecipitated from VV65T4 RDEL⁻ and VV65T4 in a 12-h pulse-chase experiment. The percentage of viral protein immunoprecipitated at 0 h (lanes 1 and 5), 4 h (lane 2), 8 h (lane 3), and 12 h (lanes 4 and 6) is shown. The intensity of the signals were determined by densitometer scanning and normalized to 100% for M-T4 RDEL⁻ (lane 1) and M-T4 (lane 5) independently.

construct the recombinant viruses VV65, VV65T4, and VV65T4 RDEL⁻. To compare levels of protein expression of VV65T4 and VV65T4 RDEL⁻, lysates from equivalent cell numbers were collected at 2, 4, 8, and 10 h p.i. Secreted proteins were also collected at 10 h p.i. Western blot analysis with the C-terminal peptide antibody (Fig. 1B) first detected M-T4 at 2 h p.i., which increased at 4 h, and was maximal by 8–10 h (Fig. 1B, lanes 3–6). No M-T4 protein is detected in the mock-infected cell or the negative control VV65 lysates (Fig. 1B, lanes 1 and 2). As in vMyxlac infection, M-T4 is also not detected in the secreted fraction (Fig. 1B, lane 7). VV65T4 RDEL⁻ expression detected by Western blot analysis with the N-terminal M-T4 antibody is somewhat different from that of VV65T4 expression, in that M-T4 RDEL⁻ is not detected at all at 2 or 4 h p.i., but maximal levels are similarly detected at 8 to 10 h (Fig. 1C, lanes 2–5). This reduced level of M-T4RDEL⁻ protein compared with M-T4 expressed from vaccinia vectors correlates with the results observed from vMyxlac and vMyxlacT4 RDEL⁻ expression as noted above.

M-T4 RDEL⁻ mutant protein exhibits reduced stability

To determine whether the altered level of M-T4 RDEL⁻ protein detected by Western blotting was due to increased protein instability, a series of pulse-chase immunoprecipitation experiments were performed. BGMK cells were mock infected or infected with vMyxlac T4⁻, vMyxlacT4 RDEL⁻, or vMyxlac, and the stability of pulse-labeled M-T4 protein was assessed (Fig. 2). After a 2-h ^{35}S labeling period, similar amounts of M-T4 RDEL⁻ and M-T4 labeled protein are detected (compare lanes 3 and 5). This suggests that the amount of *de novo* protein synthesis of both proteins is similar, and the altered expression of M-T4 RDEL⁻ is most likely due to instability of the protein at a posttranslational level. The endoglycosidase H (endo H)-sensitive analysis of the mutant M-T4 protein is discussed in the next section.

To assess the degradation of M-T4 RDEL⁻ over time, a 12-h pulse-chase immunoprecipitation experiment was performed with VV65T4 and VV65T4 RDEL⁻. BGMK cells were infected and ^{35}S Met/Cys labeled for 1 h at 8 h p.i., and the infected cells were then chased for 0, 4, 8, and 12 h. Immunoprecipitations were carried out as described in Materials and Methods. The intensities of M-T4 and M-T4 RDEL⁻ protein detected at the indicated chase times were compared and are displayed in Fig. 3. Similar amounts of M-T4 and M-T4 RDEL⁻ are present right after labeling, at time zero (insets, lanes 1 and 5). As the chase time increases, the amount of labeled M-T4

RDEL⁻ protein immunoprecipitated from infected lysates decreased dramatically from approximately 28% at 4 h to approximately 7% at 12 h (Fig. 3, lanes 2 to 4). The same trend is not observed with M-T4; M-T4 appears to be completely stable, and in fact, more labeled protein is detected at the end of the 12-h chase period (Fig. 3, lane 6), possibly because residual ^{35}S label is still present in the methionine/cysteine pools, even in the presence of cold chase. The overall trend is that M-T4 RDEL⁻ is relatively unstable and degraded by over 90% in a 12-h period, whereas no detectable degradation of wildtype M-T4 protein is observed over the same time period.

M-T4 RDEL⁻ mutant is still retained in the ER

Because Western blotting analysis indicated that M-T4 RDEL⁻ is not secreted, we wanted to more precisely determine the protein's subcellular localization. Endo H sensitivity is one way to determine whether an N-glycoprotein enters and/or leaves the ER. The ^{35}S Met/Cys-labeled M-T4 and M-T4 RDEL⁻ were immunoprecipitated from vMyxlac- and vMyxlacT4 RDEL⁻-infected cells as described above. The proteins were subjected to endo H digestion before SDS–PAGE. Both M-T4 and M-T4 RDEL⁻ become fully endo H sensitive, as observed in Fig. 2 (lanes 4 and 6), indicating that both M-T4 and M-T4 RDEL⁻ quantitatively enter the ER. To determine whether M-T4 RDEL⁻ leaves the ER to become endo H resistant, a series of pulse-chase experiments were performed. BGMK cells were infected with VV65T4 RDEL⁻ or VV65T4 and pulsed with ^{35}S Met/Cys for 1 h and then chased with cold media for 0, 4, 8, and 12 h. M-T4 and M-T4 RDEL⁻ were immunoprecipitated from these samples using the N-terminal antibody that recognizes both proteins and subjected to endo H digestion. M-T4 RDEL⁻ is still fully endo H sensitive after 8 h (Fig. 4B, lane 2), as is M-T4 as late as 12 h after labeling (Fig. 4B, lane 6). These data suggest that the remaining intact fraction of M-T4 RDEL⁻ has not exited the ER but, like M-T4, has been fully retained within this cellular compartment.

To further assess the intracellular localization of M-T4 RDEL⁻, infected BGMK cells were subjected to confocal fluorescence microscopy. Specific organelle dyes were used as internal standards to stain the ER and Golgi complex individually, and the N-terminal M-T4 peptide antibody was affinity purified and used to detect M-T4 and M-T4 RDEL⁻ protein within infected cells. To determine the intracellular localization of M-T4 and M-T4 RDEL⁻, BGMK cells were infected with VV65T4 RDEL⁻ or VV65T4, and 12 h p.i., infected cells were incubated with the ER (ER Tracker Blue-White DPX) or Golgi (BIODIPY TR ceramide) markers before fixing and permeabilization, followed by incubation with the affinity purified N-terminal M-T4 antibody and FITC-conjugated secondary antibody. Merging of M-T4- or M-T4 RDEL⁻ FITC-labeled green images (Figs. 5A and 5D) with the red dye-labeled

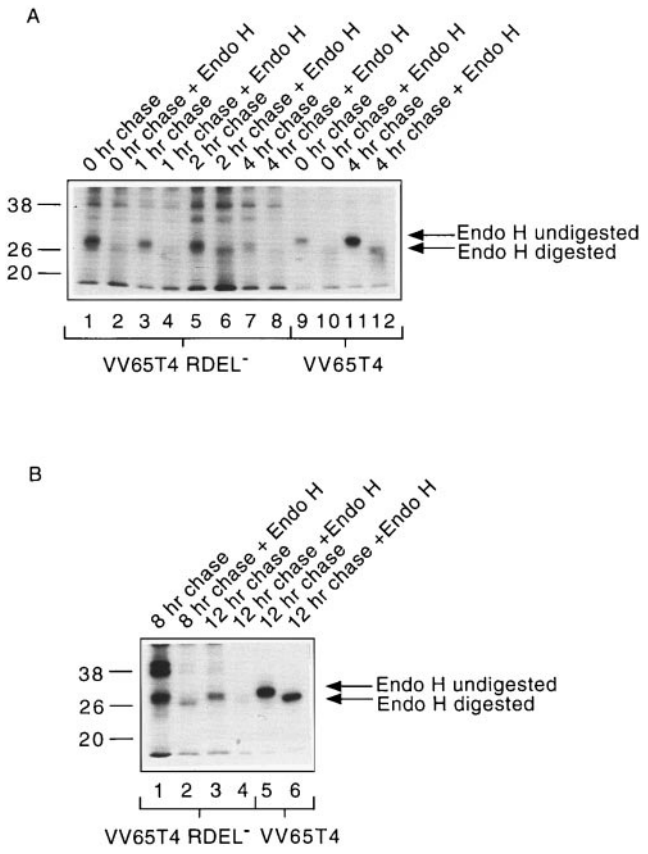

FIG. 4. Pulse-chase immunoprecipitation and endo H analysis of M-T4 RDEL⁻. (A) Four-hour pulse-chase immmunoprecipitation and endo H analysis. BGMK cells were infected with VV65T4 RDEL⁻ or VV65T4 and labeled with ^{35}S Met/Cys for 30 min at 5.5 h p.i. Samples were chased and harvested at 0 h (lanes 1, 2, 9, and 10), 1 h (lanes 3 and 4), 2 h (lanes 5 and 6), and 4 h (lanes 7, 8, 11, and 12). M-T4 RDEL protein was immunoprecipitated with antisera specific for the N-terminal of M-T4 and treated with endo H (lanes 2, 4, 6, 8, 10, and 12) before SDS–PAGE and analysis by autoradiography. (B) Twelve-hour pulse-chase immmunoprecipitation and endo H analysis. BGMK cells were infected with VV65T4 RDEL⁻ or VV65T4 and labeled with ^{35}S Met/Cys for 1 h at 8 h p.i. Samples were chased and harvested at 8 h (lanes 1 and 2) or 12 h (lanes 3, 4, 5, and 6). M-T4 RDEL⁻ protein was immunoprecipitated with antisera specific for the N-terminal of M-T4 and treated with endo H (lanes 2, 4, and 6) before SDS–PAGE and analysis by autoradiography.

Golgi apparatus (Figs. 5B and 5E) showed little colocalization as indicated by the lack of intense yellow staining on the merged images (compare Fig. 5C with Fig. 5F), indicating that neither the wildtype nor RDEL⁻ variant of M-T4 localizes to any substantial degree in the Golgi complex. Incubation of the N-terminal M-T4 antibody with cells infected with VV65, the negative control virus, showed limited background staining (not shown). In contrast, labeling infected cells with the blue ER marker dye (Figs. 5H and 5K) and FITC-conjugated M-T4 and M-T4 RDEL⁻ (shown in red in Figs. 5G and 5J) was also performed. The FITC readout was manipulated from green to red to facilitate visualization of colocalization, such that merging of the red M-T4 and M-T4 RDEL⁻

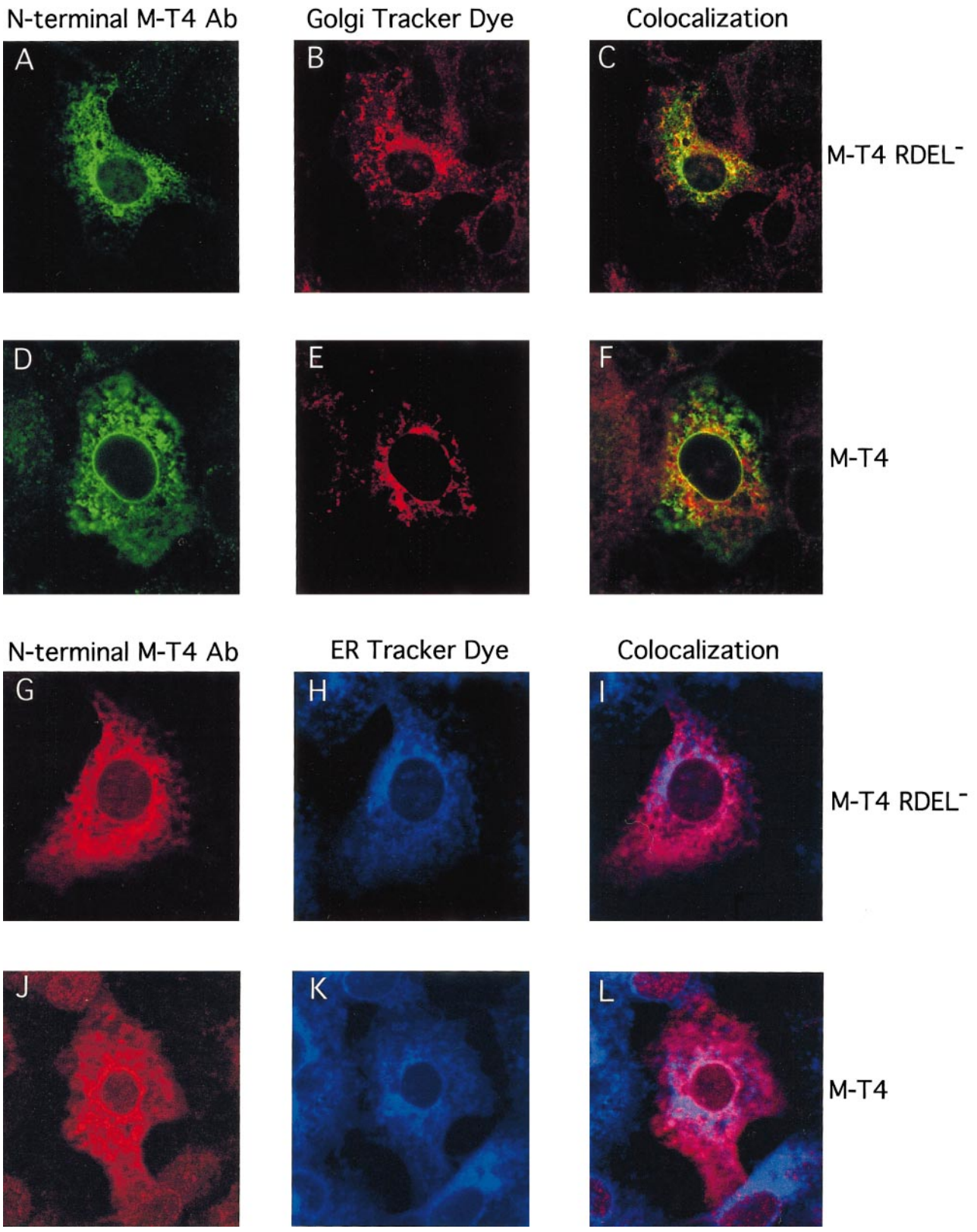

FIG. 5. M-T4 RDEL$^-$ and M-T4 colocalize with an ER marker. BGMK cells were infected with VV65T4 RDEL$^-$ (A–C and G–I) or VV65T4 (D–F and J–L) at an m.o.i. of 10 PFU/cell. At 12 h p.i., the cells were stained with a Golgi marker (red) or with an ER tracker (blue) and then fixed, permeabilized, and treated with FITC-labeled affinity purified N-terminal M-T4 antibody (green). Images of cells showing both positive green fluorescence with the N-terminal M-T4 antibody and positive red fluorescence with the Golgi marker were merged in both C and F. To visualize colocalization of the last six panels, positive green fluorescence was changed to red (G and J). Images of cells showing both positive fluorescence with the N-terminal M-T4 antibody and positive fluorescence with ER marker were merged in both I and L, and colocalization is indicated by magenta color.

proteins and the blue ER marker produces a distinctive magenta color, indicating colocalization (Figs. 5I and 5L). The levels of magenta-stained coloration were indistinguishable between the M-T4 and the M-T4 RDEL$^-$ mutant and consistent with the previous study showing colocalization of M-T4 with calreticulin in the ER (Barry *et al.,* 1997). The lack of colocalization of M-T4 RDEL$^-$ and the Golgi marker confirms the endo H results, which indicate that M-T4 RDEL$^-$ has not migrated into the Golgi complex. The colocalization of M-T4 RDEL$^-$ and the ER marker also support the previous endo H results, which suggest that both the M-T4 and M-T4 RDEL$^-$ proteins are fully retained within the ER.

vMyxlacT4 RDEL$^-$ exhibits impaired replication in a CD4$^+$ rabbit T cell line

Myxoma virus deleted for expression of M-T4 has previously been found to be defective for replication in a CD4$^+$ rabbit T cell line RL-5 and primary rabbit lymphocytes (Barry *et al.,* 1997). We were therefore interested in determining whether the mutant virus vMyxlacT4 RDEL$^-$ would behave in a similar fashion. In single-step growth curve analysis with cultured RK-13 fibroblasts cells, no defect in vMyxlacT4 RDEL$^-$ replication was observed compared with parental vMyxlac replication (Fig. 6, upper panel). However, during vMyxlacT4 RDEL$^-$ infection of the CD4$^+$ rabbit T cell line RL-5 (Fig. 6, lower panel), vMyxlacT4 RDEL$^-$ replication appears to be partially defective in RL-5 cells, intermediate between the permissive vMyxlac and the fully restricted vMyxlacT4$^-$. This indicates that the removal of the RDEL motif from M-T4, although not altering the overall localization of the protein in the ER, causes an intermediate phenotype in terms of functioning as a host range factor in lymphocytes.

Infection of lymphocytes with vMyxlacT4 RDEL$^-$ results in apoptosis

Studies with M-T5$^-$, M-T2$^-$, M11L$^-$, or M-T4$^-$ mutant myxoma viruses indicated defective viral replication in CD4$^+$ RL-5 cells because the infected cells undergo an accelerated apoptosis in response to the virus infection (Barry *et al.,* 1997; Macen *et al.,* 1996; Mossman *et al.,* 1996a). Therefore, we investigated the possibility that the reduced replication observed in RL-5 cells with vMyxlacT4 RDEL$^-$ infection was due to apoptosis.

One of the early hallmark changes in a cell undergoing apoptosis occurs at the cell surface (Andree *et al.,* 1990; Creutz, 1992; Fadok *et al.,* 1992). For example, translocation of phosphatidylserine (PS) from the inner leaflet of the plasma membrane to the outer leaflet exposes PS at the external surface of cells that are committed to apoptosis. Annexin V is a Ca^{2+}-dependent phospholipid-binding protein with high affinity for PS and can be used as sensitive probe for PS exposure on the outer leaflet of

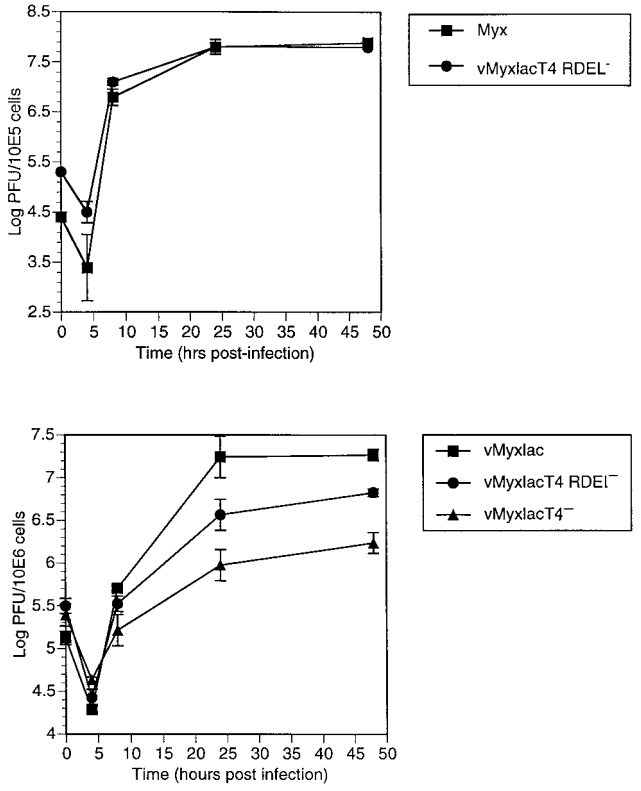

FIG. 6. Single-step growth curve analysis. The replication of vMyxlacT4 RDEL$^-$ is normal in permissive (RK-13) rabbit fibroblasts but defective in a rabbit T cell line (RL-5). RK-13 cells (A) and RL-5 cells (B) were infected with either vMyxlac, vMyxlacT4$^-$, or vMyxlacT4 RDEL$^-$ at an m.o.i. of 10. The cells were harvested at 0, 4, 8, 24, and 48 h p.i., and virus titers were determined on BGMK cells. All titrations were performed in triplicate, and standard error bars are shown.

the cell membrane of apoptotic cells (Verhoven *et al.,* 1995). Necrotic cells also expose PS due to the loss of membrane integrity, but the simultaneous application of the DNA stain propidium iodide (PI), which is not permeable to intact cells, allows the discrimination of necrotic cells from the annexin V positively stained cell cluster at early times. Despite the fact that at later stages of virus-induced apoptosis cell membrane integrity is progressively lost, thus allowing PI uptake, the assay remains useful at correlating apoptosis induction with virus replication levels of infected lymphocytes.

To determine whether RL-5 cells undergo apoptosis in response to vMyxlacT4 RDEL$^-$ infection, RL-5 cells were mock infected or infected with vMyxlac, vMyxlacT4$^-$, or vMyxlacT4 RDEL$^-$ at a multiplicity of infection (m.o.i.) of 10 PFU/cell. Cells were harvested at 4, 8, and 16 h p.i. and subjected to annexin V/PI staining. Four and 8 h were chosen as "early" time points in which annexin V-positive/PI-negative-stained cells are mostly apoptotic. We chose 16 h as a "late" time point, at which membrane integrity becomes compromised in apoptotic cells and the percent of annexin V/PI doubly positive cells increases. Mock-infected cells have a minimal single pos-

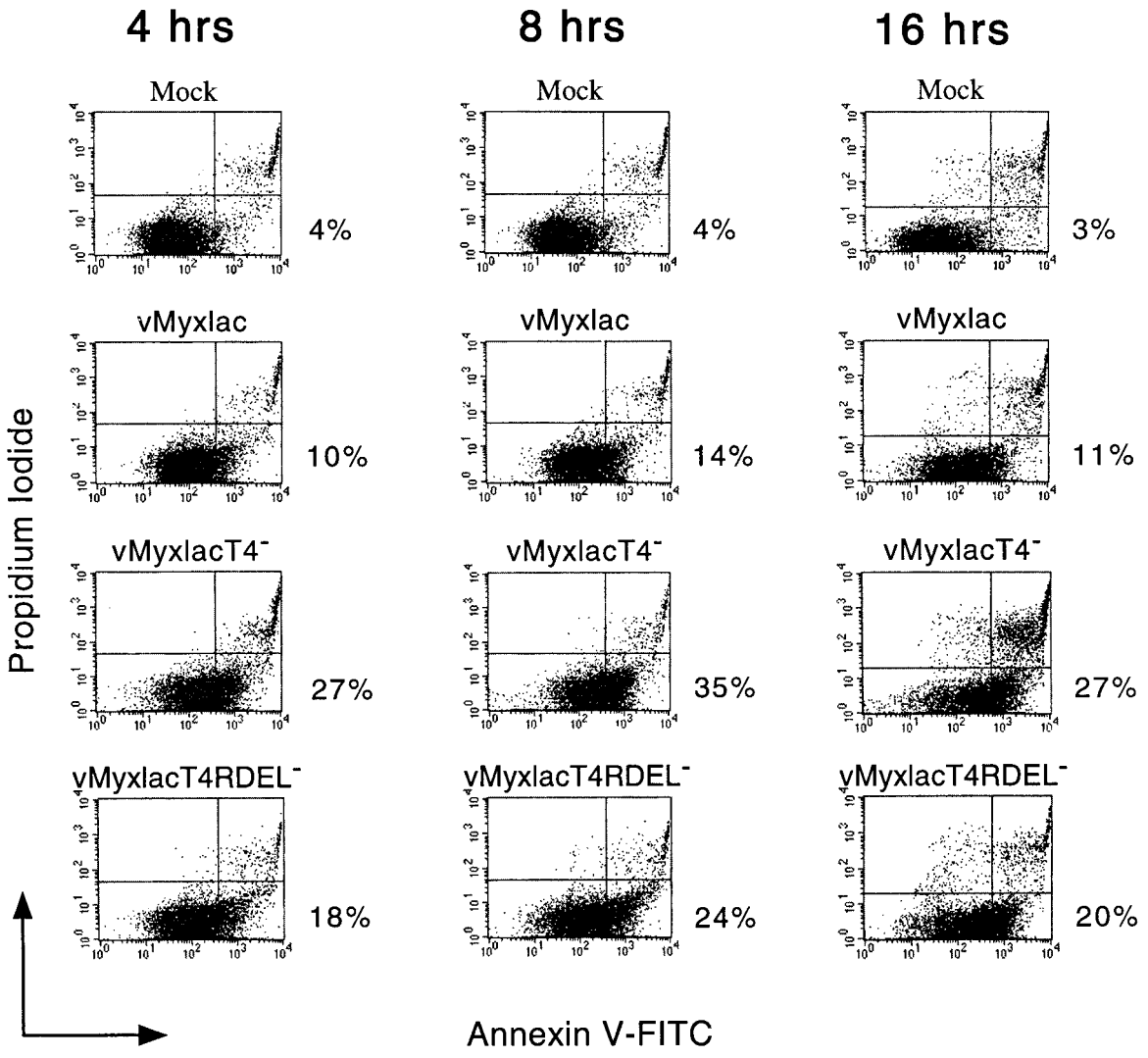

FIG. 7. Flow cytometric analysis of RL-5 cells infected with vMyxlacT4 RDEL$^-$. Flow cytometric analysis data of infected RL-5 cells. Cells were either mock infected or infected with vMyxlac, vMyxlacT4$^-$, or vMyxlacT4 RDEL$^-$ at an m.o.i. of 10 PFU/cell. At 4, 8, and 12 h p.i., the cells were harvested and stained with annexin V and PI according to Materials and Methods and subjected to FACS analysis. The percentage of annexin V-positive/PI-negative cells in the lower right quadrant of each sample is numerated. The reduction of percent values from 8 to 16 h in the virus infections corresponds to the increased leakiness of infected cells to PI.

itive annexin V staining (3–4%) at all time points (Fig. 7). Parental vMyxlac-infected cells show slightly more single positively stained annexin V cells at the time points (10–14%), which correlates with previous results using the terminal deoxynucleotidyl transferase biotin-dUTP nick end labeling assay for apoptosis-induced chromosomal fragmentation of infected RL-5 cells (Barry *et al.,* 1997; Macen *et al.,* 1996; Mossman *et al.,* 1996a). However, infection of RL-5 cells with vMyxlacT4$^-$ results in a dramatic increase of annexin V single positive cells (27–35%) compared with vMyxlac infection, which is also consistent with the previously reported DNA fragmentation assays (Barry *et al.,* 1997). The amount of single positive annexin V cells in the vMyxlacT4 RDEL$^-$ infections appears to be intermediate to that observed in vMyxlac and vMyxlacT4$^-$ infections at all time points. These data support the intermediate replication defective phenotype observed in the single-step growth curve analysis of RL-5 cells.

vMyxlacT4 RDEL$^-$ pathogenesis in European rabbits

The deletion of M-T4 from myxoma virus resulted in profound attenuation of the virus characterized by severely reduced ability of the mutant virus to migrate to secondary sites of infection (Barry *et al.,* 1997). To determine the *in vivo* effect of M-T4 RDEL$^-$ on viral virulence and pathogenesis, eight rabbits were infected with vMyxlacT4 RDEL$^-$, two rabbits were injected with parental vMyxlac, and two rabbits were injected with the M-T4 null mutant vMyxlac T4$^-$ as controls. The results of the study are shown in Table 1. Rabbits infected with vMyx-

TABLE 1

Pathogenicity of vMyxlacT4$^-$, vMyxlacT4 RDEL$^-$, and vMyxlac in Infected European Rabbits

Day	vMyxlacT4$^-$	vMyxlacT4 RDEL$^-$	vMyxlac
0	Two adult female NZW rabbits inoculated intradermally at thighs with 10^3 PFU/site	Eight adult female New Zealand White rabbits inoculated intradermally at thighs with 10^3 PFU/site	Two adult female New Zealand White rabbits inoculated intradermally at thighs with 10^3 PFU/site
3	Small primary lesions (1.5 cm) at site of inoculation, no other symptoms	Small primary lesions (1.5 cm) at site of inoculation, no other symptoms	Small primary lesions (1.5 cm) at site of inoculation, no other symptoms
5	Smaller primary lesions (1.8 cm), becoming necrotic in center of lesion	Primary lesions large (2.0–2.8 cm), swollen, necrotic centers developing; some slight discharge at nose and eyes; slight edema of head and conjunctiva; secondary lesions on ears developing	Primary lesions large (2.5–3.0 cm), swollen, necrotic centers developing; some slight discharge at nose; slight edema of head and conjunctiva; secondary lesions on ears developing
7	Primary lesion necrotic (1.5 cm), healing; small secondary lesions on ears; one rabbit with slight discharge of nose	Primary lesions large (3.5–4.0 cm), swollen, necrotic centres developing, multiple satellite lesions; secondary lesions on ears, eyes, and nose; major edema of head, conjunctiva, and slight discharge from eyes and nose; slight thickening of ears	Primary lesions large (3.5–4.0 cm), swollen, necrotic centres, multiple satellite lesions; secondary lesions on ears, eyes, and nose; major edema of head, conjunctiva, and slight discharge from eyes and nose; slight thickening of ears
9	Primary lesions regressing, necrotic; secondary lesions healing; no new lesions; no discharge from nose	Primary lesion growing (5.0 cm), multiple satellite lesions; major discharge from eyes and nose; major edema; secondary lesions growing in size and number; ears drooping, very thick, purple, and inflamed; moderate to severe bacterial infections of nasal mucosa and conjunctiva; fever; seven of eight rabbits euthanized	Primary lesions necrotic, satellite lesions; moderate/major discharge from nose and eyes; major edema; secondary lesions growing in size and number; moderate to severe bacterial infections of nasal mucosa and conjunctiva.; one of two rabbits euthanized
10–21	Both rabbits completely recovered; primary lesions and secondary lesions resolved	Final rabbit euthanized, identical phenotype as day 9	Final rabbit euthanized, identical phenotype as day 9

lacT4$^-$ showed symptoms similar to those previously described (Barry *et al.,* 1997). Briefly, the virus produced a highly attenuated disease phenotype in the rabbits, resulting in only a few small secondary lesions in the ears, no major supervening gram-negative infections, and a full recovery from the disease. In contrast, up until day 7 p.i., the symptoms of vMyxlacT4 RDEL$^-$ and vMyxlac were nearly identical. Both viruses induced large primary lesions; multiple secondary lesions on the ears, eyes, and nose; major edema of the head; slight discharge from eyes and nose; and slight thickening of the ears. However, by day 9 p.i., the vMyxlacT4 RDEL$^-$-infected rabbits had developed a novel phenotype that was particularly distinctive at secondary lesions on the ears, which became excessively edematous, swollen, deep purple in color, drooping, and excessively inflamed. vMyxlac-infected rabbits still had progressing secondary lesions on their ears, but they were not drooping and did not show evidence of such a massive proinflammatory response. Both groups of infected rabbits experienced comparable levels of severe gram-negative bacterial infections and difficulty breathing. Seven of eight vMyxlacT4 RDEL$^-$ rabbits were euthanized on day 9 due to their severe inflammatory response and respiratory complications, and one of the two vMyxlac-infected rabbit was euthanized due to respiratory complications. The final rabbits from both groups were euthanized in the following 2–4 days with severely diseased phenotypes.

Because the infection of European rabbits with vMyxlacT4 RDEL$^-$ resulted in an excessively proinflammatory myxomatosis phenotype compared with parental vMyxlac infection or null mutant vMyxlacT4$^-$ infection, additional studies were conducted to examine the nature of the inflammatory responses. Four rabbits were injected with vMyxlacT4 RDEL$^-$ or vMyxlac, and two from each group were subjected to a complete postmortem examination and histological analysis on days 5 and 9 p.i., so as to focus on secondary site lesions in the ears. Because both viruses contain the *Escherichia coli lacZ* gene, immunohistochemistry staining of these tissue sections with an antibody specific to β-galactosidase can be used to detect virally infected cells. Day 9 secondary lesion tissue sections from the ears stained with the β-galactosidase antibody reveal similar amounts of positive staining cells in both vMyxlac- and vMyxlacT4 RDEL$^-$-infected sections compared with a control ear tissue section at a site without a secondary lesion (data not shown). This suggests that vMyxlacT4 RDEL$^-$ has trafficked into and replicates within secondary sites to a comparable extent to that of vMyxlac. A final *in vivo*

TABLE 2

Summary of Histopathological Findings of Rabbit Ear Lesions on Day 9 Postinfection and Ear Thickness Measurements

Virus-infected rabbit	Epidermal/dermal thickening	Infiltrating lymphocytes	Infiltrating heterophils	Tissue necrosis	Day 0–9 Δ ear thickness
vMyxlacT4 RDEL$^-$ #1	+++	+++	+++	+++	Base: 2.0 mm Tip: 1.5 mm
vMyxlacT4 RDEL$^-$ #2	++	+++	+++	++	Base: 2.0 mm Tip: 0.5 mm
vMyxlac #1	++	+++	+	++	Base: 1.0 mm Tip: 0.5 mm
VMyxlac #2	+	+++	+	+	Base: 0.5 mm Tip: 0.5 mm

Note. +, Minimal; ++, Moderate; +++, Marked.

infection experiment was conducted to further characterize the novel phenotype observed in the ears of rabbits infected with vMyxlacT4 RDEL$^-$. In this experiment, ear thickness at the tip and base of the ear was measured daily, and as can be observed in Table 2, by day 9 p.i., rabbits infected with vMyxlacT4 RDEL$^-$ had a 2.0-mm increase in ear thickness at the base of the ear, whereas the rabbits infected with vMyxlac experienced only 0.5- to 1.0-mm increases at the base of the infected ears. A similar trend was observed at the tip of the ears of infected rabbits. The increased measure of ear thickness in rabbits infected with vMyxlacT4 RDEL$^-$ is indicative of the increased inflammation and edema observed and was typified by the dark-purple color of vMyxlacT4 RDEL$^-$-infected rabbit ears compared with wildtype (not shown). Histological analysis of ear tissues stained with hematoxylin and eosin by a third blinded party revealed a marked increase in infiltrating heterophils (likely neutrophils) in rabbits infected with vMyxlacT4 RDEL$^-$ (Table 2). A moderate increase in dermal and epidermal thickening and tissue necrosis was also observed compared with ear tissues of vMyxlac-infected rabbits. The observation of a marked increase of infiltrating heterophils correlated precisely with the increased inflammation and edema of the ears of rabbits infected with vMyxlacT4 RDEL$^-$ at the gross level.

DISCUSSION

To date, a number of myxoma virus open reading frames have been shown to be immunomodulatory regulators both *in vitro* and *in vivo* (Nash *et al.,* 1999). One of these open reading frames, myxoma virus M-T4, has previously shown to be a critical virulence factor *in vivo* and shown to have a role in protecting infected rabbit lymphocytes from apoptosis (Barry *et al.,* 1997). Interestingly, this protein contains a C-terminal RDEL motif, which has previously been demonstrated to signal for ER retention, and studies have demonstrated that M-T4 is indeed localized exclusively in the ER by confocal fluorescent light microscopy and endo H analysis (Barry *et al.,* 1997), suggesting that the C-terminal RDEL motif is critical for retrieval and retention of M-T4 in the ER.

The KDEL receptor-mediated retrograde transport system is an important retrieval mechanism by which resident soluble and membrane proteins are retained in the ER (Pelham, 1989; Pelham, 1996), and thus myxoma virus may have evolved M-T4 to use the retrograde transport system to its own benefit. Thus we decided to initiate mutational studies on the C-terminal RDEL motif of M-T4 to investigate the localization of M-T4 in the ER and its role in apoptosis. To carry out these studies, a recombinant virus vMyxlacT4 RDEL$^-$ was created in which the C-terminal RDEL motif of M-T4 was removed and a selectable marker was inserted immediately downstream of the truncated M-T4 gene.

We originally hypothesized that when the RDEL motif was removed from the protein, M-T4 would no longer be retained in the ER by retrograde transport but rather would travel through the default export pathway and possibly be secreted. However, studies of secreted proteins from cells infected with the M-T4 RDEL$^-$ mutant virus presented here demonstrate that M-T4 RDEL$^-$ is not secreted. Western blot analysis detects the predicted mutant M-T4 protein in the lysates but not in the secreted protein fractions of infected cells (Fig. 1A). These results compelled us to examine the intracellular localization of the M-T4 RDEL$^-$ mutant protein. The use of confocal fluorescent light microscopy with the aid of organelle tracker dyes determined that M-T4 RDEL$^-$, like wildtype M-T4, is still localized exclusively in the ER (Figs. 5A–5L). Immunoprecipitation and endo H digestion analysis of M-T4 RDEL$^-$ supports this finding, as both M-T4 RDEL$^-$ and wildtype M-T4 are completely endo H sensitive, even after an 8- to 12-h chase period (Figs. 4A and 4B).

There are a number of possibilities as to why M-T4 is still retained in the ER in the absence of a C-terminal RDEL motif. It has been clearly demonstrated that a C-terminal RDEL or KDEL motif signals for ER retention mediated by retrograde transport, and the addition of a C-terminal KDEL motif to a highly secreted protein or cell

surface protein results in 100% retention of the recombinant protein in the ER (Dai *et al.,* 1992; Degar *et al.,* 1996; Finley and Kornfeld, 1994; Rose-John *et al.,* 1993). Despite this, when KDEL motifs are removed from cellular ER resident proteins, the results are surprisingly variable. Removal of the C-terminal RNLL sequence from the human plasma retinol binding protein results in continued retention of the protein in the ER (Natarajan *et al.,* 1996). Prostaglandin endo H synthase-1 and -2 (PGHS-1 and -2) are ER luminal integral membrane proteins with a C-terminal S/PTEL sequence, but mutants of PGHS-1 and -2 with modified or deleted PTEL sequences were localized to the Golgi complex in transient transfection studies (Song and Smith, 1996). When the C-terminal KDEL motif is removed from calreticulin, an extensively studied soluble resident ER Ca^{2+} binding protein (Nash *et al.,* 1994), the majority of the protein is retained intracellularly, and only a fraction of the protein is secreted with very slow kinetics (M. Michalek, personal communication). Therefore, it is not completely without precedent that removal of the RDEL motif from M-T4 does not result in outright secretion of the variant protein.

One possibility for the retention of M-T4 RDEL$^-$ is that the viral protein is retained in the ER by an interaction with a cellular ER resident protein. Alternatively, the ER localization of M-T4 RDEL$^-$ could be mediated by the N-terminal signal sequence. N-terminal signal sequences direct nascent or completed proteins from the cytosol to translocation sites in the ER membrane (Martoglio and Dobberstein, 1998), after which the signal sequences can be cleaved from the protein by a membrane-bound signal peptidase. We had originally predicted that the signal sequence of M-T4 was cleaved after amino acid 28 (Barry *et al.,* 1997), but large uncleaved signal sequences with a substantial hydrophobic region can occasionally act as "signal anchor" sequences (High and Dobberstein, 1992). Thus it is possible that the M-T4 signal sequence is not actually cleaved but instead functions as a membrane anchor sequence. As an analogy of transmembrane domains that signal for ER retention, hepatitis C virus encodes two glycoproteins E1 and E2 that form a noncovalent heterodimer that accumulates in the ER (Cocquerel *et al.,* 1998; Duvet *et al.,* 1998). Studies with chimeric constructs have found that static ER retention of these glycoproteins is due to single transmembrane domains in each of the proteins (Cocquerel *et al.,* 1998).

A second important result of the study reported here is that the mutant M-T4 RDEL$^-$ protein is more unstable than the wildtype counterpart. Western blot analysis demonstrated that M-T4 RDEL$^-$ protein from the recombinant mutant virus vMyxlacT4 RDEL$^-$ is detected at a lower steady-state level than wildtype M-T4 from parental vMyxlac virus infection (Fig. 1A). Further immunoprecipitation studies, however, demonstrated that similar levels of M-T4 and M-T4 RDEL$^-$ protein are synthesized after a short pulse labeling period (Figs. 2, 3, 4A, and 4B). This suggests that the amount of *de novo* protein synthesis of both proteins is similar and that the instability of the mutant is at the protein level and not at a transcriptional or translational level. Pulse-chase experiments (Fig. 3) demonstrated that M-T4 RDEL$^-$ mutant protein has a half-life of only about 1 h, whereas in contrast, M-T4 levels do not decline even after a 12-h chase period. The cause or mechanism of the instability of M-T4 RDEL$^-$ is unknown but is presumably mediated by the chaperone-mediated degradation pathway associated with the ER.

Our initial hypothesis was that removal of the RDEL motif would cause M-T4 depletion from the ER and therefore perturb its role in apoptosis inhibition. Previous studies have shown that a recombinant virus that is null for M-T4 expression, vMyxlacT4$^-$, induced infected rabbit $CD4^+$ lymphocytes to undergo apoptosis, unlike the parental wildtype virus, vMyxlac (Barry *et al.,* 1997). Flow cytometric analysis performed to assess apoptosis levels of $CD4^+$ rabbit T lymphocytes infected with vMyxlacT4 RDEL$^-$ revealed an intermediate apoptosis phenotype compared with the vMyxlac and vMyxlacT4$^-$ infections (Fig. 7). This is a novel phenotype that can possibly be explained by the instability of the M-T4 RDEL$^-$ protein, or by altered interactions with other ER resident proteins.

Based on the biochemical data generated on the M-T4 RDEL$^-$ protein, it was difficult to predict the phenotype of the M-T4 RDEL$^-$ mutant virus *in vivo*. Initially, rabbits infected with the M-T4 RDEL$^-$ mutant virus reacted in a similar fashion to rabbits infected with the wildtype myxoma virus. Hallmark myxomatosis symptoms such as secondary lesions on the ears, nose, and eyes and gram-negative infections were typically manifest by day 7 p.i. Surprisingly, by day 9 p.i., a novel proinflammatory phenotype was noted at secondary sites in rabbits infected with the M-T4 RDEL$^-$ mutant virus. Unlike the wildtype myxoma virus infection, the ears of rabbits infected with vMyxlacT4 RDEL$^-$ underwent excessive swelling and inflammation, including colour changes from pink to a dark red/purple and pronounced edema. Histological analysis demonstrated that both the M-T4 RDEL$^-$ mutant virus and the wildtype virus effectively traveled to secondary sites of infection and replicated to comparable levels (not shown), which supported the observation of the same number of secondary lesions at the gross level between the two viruses. This contrasts with the histological and gross analysis of rabbits infected with the M-T4 null mutant virus, which displayed almost a complete absence of lesions and virus at typical secondary sites of infection. Thus unlike the M-T4 null mutant virus and like the wildtype virus, the M-T4 RDEL$^-$ mutant virus can successfully migrate through the lymphoreticular system and initiate secondary sites of infections. Hematoxylin and eosin staining of infected ear tissues displayed a clear difference between the two

virus infections. A severe inflammatory and edematous response was clearly evident in the ears of rabbits infected with the M-T4 RDEL$^-$ virus at the tissue level. Ear sections infected with the M-T4 RDEL$^-$ mutant virus displayed a marked increase in infiltrating heterophils into the tissues and a moderate increase in epidermal and dermal thickening and tissue necrosis. A massive increase in infiltrating heterophils (mostly neutrophils) into the ear tissue can account for the edema and swelling observed in the ears of infected rabbits at the gross level.

The inflammation response observed in the ears of rabbits infected with the M-T4 RDEL$^-$ virus is unexpected and is not readily explained simply by virtue of reduced stability of the mutant M-T4 protein. Historically, excessive apoptosis in tissues has been classified as a noninflammatory event. The belief that cells dying by apoptosis do not induce an inflammatory response has been supported by studies of programmed cell death during embryogenesis and development, but a recent study determined that induced apoptosis under certain circumstances can induce an inflammatory response. Inoculation of mice with tumor cells expressing Fas ligand induced a massive interleukin (IL)-1β-dependent neutrophil infiltration in wildtype mice that was suppressed in IL-1α/β knock-out mice (Miwa *et al.,* 1998). The novel phenotype observed in the ears of rabbits infected with the M-T4 RDEL$^-$ mutant virus also suggests a linkage between apoptosis and inflammation. Flow cytometric analysis demonstrated that the M-T4 RDEL$^-$ mutant virus induces an intermediate level of apoptosis in virus-infected rabbit lymphocytes. It is possible that apoptosis of infected leukocytes (possibly macrophages) in the ear tissue releases IL-1β that could be responsible for the increased heterophil infiltration observed in the ears of infected tissues.

The functional question remains: How does M-T4 protect infected cells against apoptosis from its location in the ER? There are several postulated mechanisms by which M-T4 can have a role in apoptosis that rely on the localization of M-T4 in the ER. For example, the ER is capable of detecting functional perturbations in protein and lipid concentrations and can respond by activating novel gene expression in the nucleus via a signal transduction cascade mediated by either the unfolded-protein response or the ER overload response (Chapman *et al.,* 1998). Alternatively, M-T4 could function as an antiapoptotic inhibitor by regulating the Bap31 complex in the ER. Bap31 is an ER-retained, integral membrane protein that forms a complex with Bcl-2/Bcl-x_L, procaspase 8, and other proapoptotic molecules (Ng *et al.,* 1997; Ng and Shore, 1998).

In conclusion, our studies have determined that deletion of the C-terminal RDEL motif of M-T4 does not abrogate localization to the ER but affects M-T4 stability and induces a novel proinflammatory myxomatosis phenotype. The mechanism of retention of the M-T4 RDEL$^-$ protein in the ER is unknown but could be due to protein–protein interactions and/or noncleavage of the N-terminal signal sequence. The novel myxomatosis phenotype at secondary sites of infected rabbits demonstrated an exacerbated inflammatory response, possibly due to release of proinflammatory cytokines such as IL-1β from infected macrophages. Thus it is entirely possible that M-T4 could function both as an antiapoptotic protein and as a negative regulator of proinflammatory cytokines, but the linkage between these two activities within the infected cell ER merits further investigation.

MATERIALS AND METHODS

Viruses and cells

vMyxlac used in the experiments is a derivative of myxoma virus (strain Lausanne) containing the *E. coli lacZ* gene expressed under the control of the vaccinia virus late promoter p11 inserted between the myxoma virus growth factor (MGF) and M-T9 genes (Opgenorth *et al.,* 1992a). vMyxlacT4$^-$ virus is a derivative of vMyxlac with a disruption in the M-T4 gene, and its construction has been described elsewhere (Barry *et al.,* 1997). Vaccinia virus (strain WR) was obtained from the American Type Culture Collection, and vaccinia virus (strain Copenhagen) was a gift from Dr. J. Tartaglia. VV601 is a derivative of vaccinia virus (strain WR), in which the *E. coli lacZ* gene has been inserted into the virus thymidine kinase (TK) gene under the vaccinia virus late p7.5 promoter (Macen *et al.,* 1993). VVT4 is a vaccinia virus (strain WR) construct in which the M-T4 cassette under a synthetic late vaccinia virus promoter and the *E. coli lacZ* gene under the vaccinia virus late p7.5 promoter have been inserted into the TK cassette (Barry *et al.,* 1997). vMyxlacT4 RDEL$^-$ and the recombinant vaccinia viruses VV65, VV65T4, and VV65T4 RDEL$^-$ (strain Copenhagen) construction are described below.

All viruses were propagated in a primate cell line of BGMK cells (gift from Dr. S. Dales) grown in Dulbecco's modified Eagle's medium (DMEM) supplemented with 10% newborn calf serum (NCS) (GIBCO BRL Life Technologies Inc.). Rabbit kidney RK-13 cells (American Type Culture Collection) were cultured in DMEM supplemented with 10% fetal calf serum (FCS) (GIBCO BRL Life Technologies Inc.). Rabbit lymphocyte RL-5 cells were received from the National Institutes of Health AIDS Research and Reference Reagent Program. These cells were cultured in RPMI 1640 (GIBCO BRL Life Technologies Inc.) supplemented with 10% FCS. The thymidine kinase deficient (TK$^-$) H143 cells were cultured in DMEM supplemented with 10% FCS and 25 μg/ml 5′-bromo-2′deoxyuridine (Sigma Chemical Co.) and were a gift from D. Panicali. All media was supplemented with 200 μg/ml streptomycin, 200 U/ml penicillin, and 2 mM glutamine (all from BioWhittaker Inc.).

Virus infection

Suspension cells. RL-5 cells (1×10^6) were infected with vMyxlac, vMyxlacT4$^-$, or vMyxlacT4 RDEL$^-$. The virus was infected at an m.o.i. of 10 plaque forming units (PFU)/cell, in 200 μl of medium, at 37°C. After 1 h, the suspensions were centrifuged for 10 min at 1500 rpm, and excess virus was removed by washing three times with DMEM. RPMI plus 10% FCS (2 ml) was then added to the infections, which proceeded at 37°C until the indicated times. Infected RL-5 cells were harvested by centrifugation for 10 min at 1500 rpm. Cell pellets were frozen at −80°C in 200 μl of swelling buffer (10 mM Tris, pH 8.0, 2 mM MgCl).

Adherent cells. BGMK and RK-13 cells (5×10^5) were infected with vMyxlac, vMyxlacT4$^-$, vMyxlacT4 RDEL$^-$, VV601, VVT4, VV65, VV65T4 RDEL$^-$, or VV65T4 at an m.o.i. of 10 PFU/cell. Virus was incubated in 300 μl of DME plus 10% NCS or FCS (BGMK cells or RK-13 cells, respectively) on monolayers for 1 h at 37°C; then excess virus was removed by washing the monolayer three times with DMEM. Fresh medium was added, and the infections were allowed to proceed until the given times. Infected BGMK and RK-13 cells were harvested by first washing the monolayer with 1× SSC (0.15 M NaCl, 0.015 M sodium citrate). Trypsin (0.25%) (BioWhittaker Inc.) diluted in 1× SSC was added directly to the cells for 5 min at 37°C to detach the monolayers. The infected cells were centrifuged for 5 min at 1500 rpm and resuspended in swelling buffer before freezing at −80°C.

Construction of vMyxlacT4 RDEL$^-$ mutant virus

To construct the vMyxlacT4 RDEL$^-$ virus in which the C-terminal amino acid RDEL motif is removed from the M-T4 open reading frame, vMyxlac viral DNA was harvested and used as a template for PCR amplification. Viral DNA (500 ng) was subjected to the following program in a Minicycler PCR machine (MJ Research), Program 1: step 1, 6 min at 95°C; step 2, 1.5 min at 95°C; step 3, 1.5 min at 45°C; step 4, 3 min at 72°C; step 5, return to step 2 35 times; and step 6, 10 min 72°C. The 5′ region of M-T3 was amplified with primers RDEL.1 (5′-TTACGAGATCTAGTAGCAATATCAGGCATTTTCACG) and RDEL.2 (5′-CGTATCGCGTAAAAGACGAA). The 3′ region of M-T4 up to but not including the RDEL motif was amplified with primers RDEL.3 (5′-CTACTAGATCTCGTAATTATAATACTTTTGCGACGTAGG) and RDEL.4 (5′-TTAATCGACACGTCGTGCGT). The M-T4 native stop codon was designed to follow the coding sequence in primer RDEL.3, and a *Bgl*II restriction site was engineered at the 3′ end of primer RDEL.3 and the 5′ end of RDEL.1 to facilitate cloning of a *Bgl*II *E. coli* gpt cassette that is under control of the vaccinia virus p7.5 promoter (Falkner and Moss, 1988). A slow anneal PCR (Program 2: step 1, 2 min at 95°C; step 2, 1°C/min to 40°C; step 3, 3 min at 72°C) with primers RDEL.2 and RDEL.4, followed by PCR with Program 1 resulted in a 400-bp fragment that consisted of the 3′ of M-T4 without the RDEL motif and the 5′ of M-T3. This PCR fragment was cloned into a pT7Blue T-vector (Novagen), creating the plasmid pT7Blue-T4RDEL$^-$. This construct was subjected to DNA automated sequencing (Sequencing Facility, The John P. Robarts Research Institute) to ensure sequence fidelity before proceeding. The gpt cassette was cloned into the engineered *Bgl*II cassette, creating the plasmid pT7BlueT4RDEL$^-$gpt.

The plasmid pT7BlueT4RDEL$^-$gpt and vMyxlac were used to construct the recombinant virus vMyxlacT4 RDEL$^-$ by a method previously described (Mossman *et al.,* 1996a,b). To confirm construction of the recombinant virus, PCR analysis with primers RDEL.4 and RDEL.2 was performed, as described above.

Construction of M-T4 expressing vaccinia virus variants

VV601 (control) and VVT4 (expressing M-T4) are recombinant vaccinia viruses (strain WR) in which the viral TK gene has been interrupted by the *E. coli lacZ* gene, which is under the vaccinia virus late p7.5 promoter, and a vaccinia virus synthetic late promoter drives expression of the empty cassette (VV601) (Macen *et al.,* 1993) or M-T4 (VVT4) (Barry *et al.,* 1997). Three novel recombinant vaccinia viruses were constructed from strain Copenhagen using the plasmid pSC65, which contains a genetically engineered synthetic early-late viral promoter (Chakrabarti *et al.,* 1997). The method used to create the recombinant viruses was previously described (Macen *et al.,* 1993). To generate the VV65T4 RDEL$^-$ recombinant virus, the entire M-T4 open reading frame lacking the C-terminal amino acid RDEL motif was obtained by PCR analysis (as described above) with primer T4.1 (5′-CATATGAAAATGTACACGCGATTATC) (Barry *et al.,* 1997) and primer RDEL.KO (5′-TTATTATAATACTTTTGCTGACGTAGGGC), in which the codon for arginine (R) in the RDEL motif has been replaced with a stop codon. For VV65T4, PCR analysis of M-T4 was carried out as previously described (Barry *et al.,* 1997). The PCR fragments were then subcloned into the cloning vector pT7Blue3 (Novagen) and confirmed by automated DNA sequencing (Sequencing Facility, The John P. Robarts Research Institute). The M-T4 RDEL$^-$ and M-T4 cassettes were then cloned into the *Kpn*I and *Sal*I sites of the pSC65 vector, which placed the cassettes under a synthetic early/late promoter. pSC65, pSC65+T4, and pSC65+T4 RDEL$^-$ were each transfected into vaccinia virus (strain Copenhagen)-infected cells to produce the recombinant viruses VV65, VV65T4 RDEL$^-$, and VV65T4, respectively. PCR and Western blot analysis (as described below) were performed to ensure correct construction of the recombinant viruses.

Preparation M-T4 antiserum

To generate an N-terminal M-T4 specific antibody, a peptide was synthesized that consists of the first 10 amino acids of M-T4 past the predicted N-terminal signal sequence (YVIDPCTSQE) (Alberta Peptide Institute, University of Alberta, Canada). Two rabbits were immunized by injection of 500 μg of peptide conjugated to keyhole limpet hemacyanin and dissolved in 0.5 ml of PBS and 0.5 ml of Freund's complete adjuvant (Sigma Chemical Co.). The rabbits received a boost of 500 μg of antigen in Freund's incomplete adjuvant (Sigma Chemical Co.) 2 weeks after the initial injection. Two weeks after the boost, a serum sample was taken from the animals, and the presence of antibody specific to M-T4 was tested via Western blotting analysis (see below). Boosts and serum samples were repeated three additional times, and then total serum was collected from both rabbits.

The C-terminal peptide antibody is a polyclonal rabbit antibody that recognizes the last 10 amino acid residues, including the RDEL, of M-T4 (Barry *et al.,* 1997).

Western blotting analysis

To detect M-T4 and M-T4 RDEL$^-$ protein, BGMK cells (1×10^6) were infected with vMyxlac, vMyxlacT4$^-$, vMyxlacT4 RDEL$^-$, VV65, VV65T4, or VV65T4 RDEL$^-$ at an m.o.i. of 10 PFU/cell. After a 1-h infection at 37°C, the monolayers were washed with serum-free medium to remove excess virus. Fresh serum free DMEM was added to infections that proceeded until indicated times. Virally infected cellular lysates were collected by directly harvesting the cells into 100 μl of 1× SDS–PAGE loading buffer at the indicated times. Proteins secreted from infected cells were centrifuged at 12,000 *g* for 15 min to pellet debris and then concentrated fourfold by precipitation with 5 volumes of ice cold acetone or 50-fold with spin microconcentrators (Millipore). All samples were resolved by 12% SDS–PAGE. Proteins were transferred to HyBond-C-supported nitrocellulose (Amersham Inc.) via a semidry transfer apparatus (Tyler Corp.) at 100 mA for 2 h. Membranes were blocked in 5% skim milk powder containing PBS and 0.1% Tween 20 for 16 h. The C-terminal M-T4 peptide antibody was used at 1:10,000 dilution, the N-terminal M-T4 peptide antibody was used at 1:2000, and the M-T7 polyclonal antibody (Lalani *et al.,* 1997) was used at 1:5000. All antibodies were incubated with the nitrocellulose for 2 h, followed by three 5-min washes with PBS plus 0.1% Tween 20. The membranes were then incubated with horseradish peroxidase-conjugated goat anti-rabbit secondary antibody (Jackson ImmunoResearch Laboratories) at 1:5000 dilution for 1 h, and the washes repeated. Proteins were visualized using enhanced chemiluminescence (NEN Life Science Products Inc.) and Kodak film (NEN Life Science Products Inc.).

Immunoprecipitations and endo H analysis

BGMK cells (5×10^6) were infected with vMyxlac, vMyxlacT4$^-$, or vMyxlacT4 RDEL$^-$ at an m.o.i. of 10 PFU/cell. Infected monolayers were washed with DMEM Met-Cys- media (ICN), supplemented with 2 mM glutamine. Infected cells were then incubated in this media for 30 min before the addition of 500 μCi of [^{35}S]Cys/[^{35}S]Met (ICN) for 2 h at 2–4 or 4–6 h p.i. All samples were washed with PBS before lysis in Nonidet P-40 lysis buffer containing 150 mM NaCl, 50 mM Tris–HCl, pH 8.0, 1% Nonidet P-40, 1 mM phenylmethylsulfonyl fluoride, and a Complete Mini (protease inhibitor cocktail tablet) (Boehringer Mannheim) for 30 min at 4°C with agitation. Lysates were cleared of nuclei by centrifugation at 12,000 *g* for 15 min, and then the N-terminal M-T4 antibody was added to the lysates at 1:50 dilution and incubated overnight with agitation at 4°C. A 50% (100 μl) slurry of protein A–Sepharose beads (Pharmacia Biotech) was added for 1 h at 4°C with agitation. The beads were collected by 30-s centrifugation and washed three times with Nonidet P-40 lysis buffer. In the samples to undergo endo H_f digestion, beads were resuspended in denaturing buffer, and the protein was denatured by boiling for 10 min in 0.5% SDS and 0.1% 2-mercaptoethanol (BDH Laboratory Supplies). The denaturing buffer was neutralized by the addition of 50 mM sodium citrate, pH 5.5, before the addition of 2000 U of endo H_f (New England Biolabs). Digestion occurred for 1 h at 37°C, and the reaction was terminated by the addition of equal volume of SDS–PAGE gel loading buffer. Those samples not undergoing endo H_f digestion had SDS–PAGE gel loading buffer added directly to washed beads. All samples were boiled for 10 min before 12% SDS–PAGE. Resolved SDS–PAGE gels were incubated for 30 min with Amplify (Amersham Pharmacia Biotech), dried for 30 min with a model 583 Gel Dryer (Bio-Rad), and then subjected to autoradiography with Kodak film.

For the 4-h pulse-chase experiment, BGMK cells (5×10^5) were infected with VV65T4 RDEL$^-$ and VV65T4 at an m.o.i. of 10 PFU/cell for 5.5 h at 37°C. Monolayers were then washed and depleted of methionine and cysteine as above. A pulse of 500 μCi of [^{35}S]Cys/[^{35}S]Met (ICN) was added to the infected cells for 30 min at 37°C. The cells were then washed with DMEM to remove the radioactivity, DME plus 20% NCS was added back to the cells, and the infections were allowed to proceed for the designed chase times (0, 1, 2, and 4 h) and then harvested as above. For the 12-h pulse-chase experiment, the infection was allowed to proceed for 8 h before depletion of the cells of cysteine and methionine for 30 min, followed by pulsing with 500 μCi of [^{35}S]Cys/[^{35}S]Met for 1 h. The infected monolayers were washed, and medium was added back to the infections as above until the designated harvest times.

To analyze protein degradation, the intensity of M-T4

and M-T4 RDEL$^-$ protein bands from the pulse-chase experiments above was analyzed using a FX Molecular Imaging System (Bio-Rad).

Detection of apoptosis

Flow cytometric analysis with Annexin-V-Fluos (Boehringer Mannheim) and PI (Sigma Chemical Co.) was performed to detect apoptosis of virally infected rabbit lymphocytes. RL-5 cells (5×10^5) were mock infected or infected with vMyxlac, vMyxlacT4$^-$, or vMyxlacT4 RDEL$^-$ at an m.o.i. of 10 PFU/cell. At 4, 8, and 16 h p.i., the cells were harvested and washed once with PBS. The cell pellets were then resuspended in 50 μl of incubation buffer (10 mM HEPES/NaOH, pH 7.4, 140 mM NaCl, 5 mM $CaCl_2$) with PI (1 μg/ml) and Annexin-V-Fluos (2 ng/μl). Incubation buffer (450 μl) was added to all samples before analysis on a flow cytometer using 488-nm excitation and a 515-nm bandpass filter for fluorescein detection and a filter of more than 560 nm for PI detection. Results were viewed using Cellquest software.

Single-step growth curve analysis and virus titration

RK-13 cells (5×10^5) were infected with vMyxlac and vMyxlacT4 RDEL$^-$, and RL-5 cells (1×10^6) were infected with vMyxlac, vMyxlacT4$^-$, and vMyxlacT4 RDEL$^-$ in triplicate at an m.o.i. of 10 PFU/cell for 1 h. After a 1-h infection at 37°C, cells were washed three times with DMEM to remove excess virus. Infected cells were harvested at 0, 4, 8, 24, and 48 h p.i. for all virus infections in both cell lines, and viral titers were determined by foci formation on BGMK cells as previously described (Opgenorth *et al.,* 1992a).

vMyxlacT4 RDEL$^-$ pathogenesis

Adult female New Zealand White rabbits (*Oryctolagus cuniculus*) were purchased from a local supplier and housed in a Biohazard Level III containment facility in accordance with guidelines published by the Canadian Council on Animal Care. Rabbits were injected intradermally in each thigh with 10^3 PFU/site of virus. Initially, eight rabbits received vMxylacT4 RDEL$^-$ injections, two received the parental virus vMyxlac, and two received vMyxlacT4$^-$ injections so we could observe and compare the progression of the disease between the three viruses. The rabbits were monitored daily for clinical symptoms of myxomatosis and were euthanized with an injection of Euthanal when they exhibited an extreme myxomatosis phenotype. For histological analysis, a second set of eight rabbits was infected. Four rabbits received vMyxlacT4 RDEL$^-$ and four received vMyxlac injections. Two rabbits from each group were sacrificed on days 5 and 9 p.i. and subjected to a complete postmortem examination. Spleen, lymph node, primary lesions, and secondary lesions were harvested from the animals and preserved in 10% buffered Formalin. A third set of four rabbits was infected to further assess the disease symptoms manifested in the ears. Two rabbits received vMyxlacT4 RDEL$^-$ and two received vMyxlac injections as described. Photographs of the rabbits and ear thickness measurements with a caliber were recorded daily. All animals were euthanized on day 9 p.i., some due to the severity of the disease, and a single ear from each rabbit was fixed in 10% buffered Formalin.

Histological analysis

All tissue sections harvested from the eight rabbits subjected to postmortem analysis, and the ear tissues from the third myxomatosis experiment were embedded in paraffin, cut into 5-μm sections, and stained with hematoxylin and eosin for viewing by light microscope (Mossman *et al.,* 1996b). For immunohistochemical analysis, the tissue sections were rehydrated by standard procedure: deparafinize by heating sections at 60°C for 30 min, followed by 10-min incubations in xylene solutions. Sections were then washed with PBS and blocked with 20% normal horse serum (Vector Laboratories) for 15 min in a humidified chamber at room temperature. Mouse anti-β-galactosidase antibody (Promega) at a 1:500 dilution was added directly to the tissues and incubated overnight at 4°C in the humidified chamber. Sections were then washed with PBS, and biotinylated anti-mouse IgG (H+L) affinity-purified antibody (Vector Laboratories) at 1:200 was added directly to tissues for 20 min at room temperature in the humidified chamber. Sections were washed with PBS and quenched in 3% H_2O_2 in methanol for 5 min followed by a PBS wash. Avidin Biotin Complex (ABC) Elite solution (Vector Laboratories) was incubated on tissues for 40 min at room temperature. Sections were then washed with PBS, and colour was developed with 3,3′-diaminobenzidine tablets (Sigma Chemical Co.) for 30 s to 5 min. The reaction was stopped by rinsing sections with water for 10 min before hematoxylin staining and dehydration. Finally, samples were mounted in Permount and photographed using Kodak Ektachrome 64T color reversal film and Northern Eclipse software.

Affinity purification of N-terminal M-T4 antibody

Nitrocellulose-bound antigen affinity purification was used to purify the polyclonal N-terminal M-T4 antibody (Peralta *et al.,* 1993). Briefly 10 μg of the peptide YVIDPCTSQE conjugated to bovine serum albumin was loaded onto 12% SDS–PAGE and transferred to nitrocellulose as described above. The membrane was washed in PBS plus 0.4% Tween before staining with India Ink at room temperature for 18 h. The dark band observed on the membrane corresponding to the BSA-conjugated peptide was cut from the membrane into 0.5-cm squares. The squares were then blocked with TBS (Tris-buffered saline) plus 1% ovalbumin, 50 mM Tris–HCl, pH 7.0, and

150 mM NaCl for 16 h at 4°C with agitation. Blocking solution was removed, and 1:100 dilution of the original polyclonal antisera in blocking media was incubated with the squares for 16 h at room temperature with agitation. The squares were then washed three times with TBS, and then affinity-purified antibody was eluted twice with 0.1 M glycine/HCl, pH 2.5, plus 0.1% ovalbumin. The elution was immediately diluted with 0.25 volume of 1 M Tris, pH 7.5, and stored at 4°C.

Immunofluorescence and confocal microscopy

BGMK cells (2×10^5) were grown directly onto 1-mm coverslips (Fisher Scientific Company) and infected with either VV65T4 RDEL$^-$ or VV65T4 at an m.o.i. of 10 PFU/cell for 12 h. The Golgi complex and ER were visualized using the organelle specific BIODIPY TR ceramide *N*-((4-(4,4-difluoro-5-(2thienyl)-4bora-3a,4a-diaza-s-indacene-3-yl)phenoxy)acetyl)sphingosine or ER Tracker Blue-White DPX (Molecular Probes), respectively. The infected BGMK cells were incubated with 2 μM BIODIPY TR in fresh prewarmed media for 30 min at 37°C, followed by incubation with fresh medium for 20 min to allow accumulation of the stain in the Golgi complex. ER Tracker Blue-White DPX (2 μM) in fresh prewarmed media was incubated on infected cells for 50 min at 37°C. The coverslips were then washed with PBS containing 1% FCS and fixed with 2% paraformaldehyde for 20 min at room temperature. The cells were washed again with PBS plus 1% FCS and permeabilized by incubation on ice for 2 min with ice-cold 1% Triton-X (BDH Laboratory Supplies). The cells were washed as before and blocked with PBS containing 1% FCS, 3% normal goat serum (Gibco BLR Life Technologies), and 50 mM ammonium chloride for 20 min at 37°C. Affinity purified N-terminal M-T4 antibody was then added at 1:10 dilution directly to the coverslips for 1 h at room temperature. The coverslips were then washed, and donkey anti-rabbit FITC-conjugated secondary antibody was added at 1:250 dilution for 30 min at room temperature. The coverslips were washed once more and mounted in 0.01% *p*-phenylenediamine (Sigma Chemical Co.) to prevent photobleaching before analysis by confocal fluorescence microscopy. Confocal fluorescence microscopy was performed at The University of Western Ontario Department of Anatomy and Cell Biology confocal laser scanning microscope facility, and data were analyzed using Carl Zeiss LSM software.

ACKNOWLEDGMENTS

We are grateful to J. Barrett, A. S. Lalani, and J. Cao for assistance with the animal studies; L. Chen for expert technical support; and X.-M. Xu for scientific advice. We would also like to thank D. Elias for her invaluable administrative support and H. Everett and A. S. Lalani for critical comments on the manuscript. This work was funded by the Medical Research Council of Canada (MRC) and the National Cancer Institute of Canada. G.M. holds an MRC Senior Scientist Award, M.B. was a recipient of a Post-Doctoral Award from the Alberta Heritage Foundation for Medical Research, and S.H. was funded by an Ontario Graduate Scholarship, The John P. Robarts Research Institute Graduate Student Award, and The University of Ontario Special University Scholarship.

REFERENCES

Andree, H., Reutelingsperger, C. P., Hauptmann, R., Hemker, H. C., Hermens, W. T., and Willems, G. M. (1990). Binding of vascular anticoagulant alpha VAC alpha to planar phospholipid bilayers. *J. Biol. Chem.* **265,** 4923.

Barry, M., Hnatiuk, S., Mossman, K., Lee, S.-F., Boshkov, L., and McFadden, G. (1997). The myxoma virus M-T4 gene encodes a novel RDEL-containing protein that is retained within the endoplasmic reticulum and is important for the productive infection of lymphocytes. *Virology* **239,** 360–377.

Chakrabarti, S., Sisler, J. R., and Moss, B. (1997). Compact, synthetic, vaccinia virus early/late promoter for protein expression. *BioTechniques* **23,** 1094–1097.

Chapman, R., Sidrauski, C., and Walter, P. (1998). Intracellular signaling from the endoplasmic reticulum to the nucleus. *Annu. Rev. Cell Dev. Biol.* **14,** 459–485.

Cocquerel, L., Meunier, J.-C., Pillez, A., Wychowski, C., and Dubuisson, J. (1998). A retention signal necessary and sufficient for endoplasmic reticulum localization maps to the transmembrane domain of hepatitis C virus glycoprotein E2. *J. Virol.* **72,** 2183–2191.

Creutz, C. E. (1992). The annexins and exocytosis. *Science* **258,** 924.

Dai, Z., Stiles, A., Moats-Staats, B., Van Wyk, J. J., and D'Ercole, A. J. (1992). Interaction of secreted insulin-like growth factor-1 (IGF-1) with cell surface receptors is the dominant mechanism of IGF-1's autocrine actions. *J. Biol. Chem.* **267,** 19565–19571.

Degar, S., Johnson, E., Boritz, E., and Rose, J. (1996). Replication of primary HIV-1 isolates is inhibited in PM1 cells expressing sCD4-KDEL. *Virology* **226,** 424–429.

Duvet, S., Cocquerel, L., Pillez, A., Cacan, R., Verbert, A., Moradpour, D., Wychowski, C., and Dubuisson, J. (1998). Hepatitis C virus glycoprotein complex localization in the endoplasmic reticulum involves a determinant for retention and not retrieval. *J. Biol. Chem.* **273,** 32088–32095.

Fadok, V., Voelker, D. R., Campbell, P. A., Cohen, J. J., Bratton, D. L., and Henson, P. M. (1992). Exposure of phosphatidylserine on the surface of apoptotic lymphocytes triggers specific recognition and removal by macrophages. *J. Immunol.* **148,** 2207.

Falkner, F. G., and Moss, B. (1988). *Escherichia coli* gpt gene provides dominant selection for vaccinia virus open reading frame expression vectors. *J. Virol.* **62,** 1849–1854.

Fenner, F., and Ratcliffe, F. N. (1965). "Myxomatosis." Cambridge University Press, Cambridge, UK.

Fenner, F., and Ross, J. (1994). Myxomatosis. *In* "The European Rabbit: The History and Biology of a Successful Colonizer" (G. V. Thompson and C. M. King, Eds.), pp. 205–239. Oxford University Press, Oxford/New York/Tokyo.

Finley, E., and Kornfeld, S. (1994). Subcellular localization and targeting of cathepsin E. *J. Biol. Chem.* **269,** 31259–31266.

Graham, K. A., Lalani, A. S., Macen, J. L., Ness, T. L., Barry, M., Liu, L.-Y., Lucas, A., Clark-Lewis, I., Moyer, R. W., and McFadden, G. (1997). The T1/35kDa family of poxvirus secreted proteins bind chemokines and modulate leukocyte influx into virus infected tissues. *Virology* **229,** 12–24.

High, S., and Dobberstein, B. (1992). Mechanisms that determine the transmembrane disposition of proteins. *Curr. Opin. Cell Biol.* **4,** 581–586.

Lalani, A. S., Masters, J. M., Graham, K. A., Liu, L.-Y., Lucas, A., and McFadden, G. (1999). The role of the myxoma virus soluble CC-chemokine inhibitor glycoprotein, M-T1, during myxoma virus pathogenesis. *Virology* **256,** 233–245.

Lalani, A. S., Ness, T. L., Singh, R., Harrison, J. K., Seet, B. T., Kelvin, D. J., McFadden, G., and Moyer, R. W. (1998). Functional comparisons among members of the poxvirus T1/35kDa family of soluble CC-chemokine inhibitor glycoproteins. *Virology* **250,** 173–184.

Macen, J. L., Graham, K. A., Lee, S. F., Schreiber, M., Boshkov, L. K., and McFadden, G. (1996). Expression of the myxoma virus tumor necrosis factor receptor homologue (T2) and M11L genes is required to prevent virus-induced apoptosis in infected rabbit T lymphocytes. *Virology* **218,** 232–237.

Macen, J. L., Upton, C., Nation, N., and McFadden, G. (1993). SERP-1, a serine proteinase inhibitor encoded by myxoma virus, is a secreted glycoprotein that interferes with inflammation. *Virology* **195,** 348–363.

Martoglio, B., and Dobberstein, B. (1998). Signal sequences: More than just greasy peptides. *Trends Cell Biol.* **8,** 410–415.

McFadden, G., and Barry, M. (1998). How poxviruses oppose apoptosis. *Semin. Virol.* **8,** 429–442.

McFadden, G., and Graham, K. (1994). Modulation of cytokine networks by poxviruses: The myxoma virus model. *Semin. Virol.* **5,** 421–429.

McFadden, G., Graham, K., Ellison, K., Barry, M., Macen, J., Schreiber, M., Mossman, K., Nash, P., Lalani, A., and Everett, H. (1995). Interruption of cytokine networks by poxviruses: Lessons from myxoma virus. *J. Leukoc. Biol.* **57,** 731–738.

Miwa, K., Asano, M., Horai, R., Iwakura, Y., Nagata, S., and Suda, T. (1998). Caspase 1-independent IL-1β release and inflammation induced by the apoptosis inducer Fas ligand. *Nat. Med.* **258,** 511–516.

Mossman, K., Lee, S. F., Barry, M., Boshkov, L., and McFadden, G. (1996a). Disruption of M-T5, a novel myxoma virus gene member of the poxvirus host range superfamily, results in dramatic attentuation of myxomatosis in infected European rabbis. *J. Virol.* **70,** 4394–4410.

Mossman, K., Nation, P., Macen, J., Garbutt, M., Lucas, A., and McFadden, G. (1996b). Myxoma virus M-T7, a secreted homolog of the interferon-γ receptor, is a critical virulence factor for the development of myxomatosis in European rabbits. *Virology* **215,** 17–30.

Mossman, K., Upton, C., and McFadden, G. (1995). The myxoma virus soluble interferon-γ receptor homolog, M-T7, inhibits interferon-γ in a species specific manner. *J. Biol. Chem.* **270,** 3031–3038.

Nash, P., Barrett, J., Cao, J.-X., Hota-Mitchel, S., Lalani, A. S., Everett, H., Xu, X.-M., Robichaud, J., Hnatiuk, S., Ainslie, C., Seet, B., and McFadden, G. (1999). Immunomodulation by viruses: The myxoma virus story. *Immunol. Rev.* **168,** 103–120.

Nash, P., Lucas, A., and McFadden, G. (1997). SERP-1, a poxvirus-encoded serpin, is expressed as a secreted glycoprotein that inhibits the inflammatory response to myxoma virus infection. *In* "Chemistry and Biology of Serpins" (F. C. Church, D. D. Cunningham, D. Ginsburg, M. Hoffman, S. R. Stone, and D. M. Tollefsen, Eds.), pp. 195–205. Oxford University Press, New York.

Nash, P., Opas, M., and Michalek, M. (1994). Calreticulin: Not just another calcium binding protein. *Mol. Cell Biochem.* **135,** 71–78.

Nash, P., Whitty, A., Handwerker, J., Macen, J., and McFadden, G. (1998). Inhibitory specificity of the anti-inflammatory myxoma virus serpin, Serp-1. *J. Biol. Chem.* **273,** 20982–20991.

Natarajan, V., Holven, K., Reppe, S., Blomhoff, R., and Moskaug, J. O. (1996). The C-terminal RNLL sequence of the plasma retinol-binding protein is not responsible for its intracellular retention. *Biochem. Biophys. Res. Commun.* **221,** 374–379.

Ng, F. W. H., Nguyen, M., Kwan, T., Branton, P. E., Nicholson, D. W., Cromlish, J. A., and Shore, G. C. (1997). p28Bap31, a bcl-2/bcl-X_L-and procaspase-8-associated protein in the endoplasmic reticulum. *J. Cell. Biol.* **139,** 327–338.

Ng, F. W. H., and Shore, G. C. (1998). Bcl-X_L cooperatively associates with the Bap31 complex in the endoplasmic reticulum, dependent on procaspase-8 and Ced-4 adaptor. *J. Biol. Chem.* **273,** 3140–3143.

Nilsson, T., and Warren, G. (1994). Retention and retrieval in the endoplasmic reticulum and the Golgi apparatus. *Curr. Opin. Cell Biol.* **6,** 517–521.

Opgenorth, A., Graham, K., Nation, N., Strayer, D., and McFadden, G. (1992a). Deletion analysis of two tandemly arranged virulence genes in myxoma virus, M11L and myxoma growth factor. *J. Virol.* **66,** 4720–4731.

Opgenorth, A., Strayer, D., Upton, C., and McFadden, G. (1992b). Deletion of the growth factor gene related to EGF and TGF α reduces virulence of malignant rabbit fibroma virus. *Virology* **186,** 175–191.

Pelham, H. R. B. (1989). Control of protein exit from the endoplasmic reticulum. *Annu. Rev. Cell Biol.* **5,** 1–23.

Pelham, H. R. B. (1990). The retention signal for soluble proteins of the endoplasmic reticulum. **15,** 483–486.

Pelham, H. R. B. (1996). The dynamic organization of the secretory pathway. *Cell Struct. Funct.* **21,** 413–419.

Peralta, D., Lithgow, T., Hoogenraad, N. J., and Hoj, P. B. (1993). Prechaperonin 60 and preornithine transcarbamylase share components of the import apparatus but have distinct maturation pathways in rat liver mitochondria. *Eur. J. Biochem.* **211,** 881–889.

Ploegh, H. L. (1998). Viral strategies of immune evasion. *Science* **280,** 248–253.

Rose-John, S., Schooltink, H., Schmitz-Van de Leur, H., Mullberg, J., Heinrich, P., and Graeve, L. (1993). Intracellular retention of interleukin-6 abrogates signaling. *J. Biol. Chem.* **268,** 22084–22091.

Schreiber, M., and McFadden, G. (1994). The myxoma virus TNF-receptor homologue inhibits TNFα in a species specific fashion. *Virology* **204,** 692–705.

Schreiber, M., Sedger, L., and McFadden, G. (1997). Distinct domains of M-T2, the myxoma virus TNF receptor homolog, mediate extracellular TNF binding and intracellular apoptosis inhibition. *J. Virol.* **71,** 2171–2181.

Smith, G. L. (1994). Virus strategies for evasion of the host response to infection. *Trends Microbiol.* **2,** 81–88.

Smith, G. L., Symons, J. A., Khanna, A., Vanderplasschen, A., and Alcamí, A. (1997). Vaccinia virus immune evasion. *Immunol. Rev.* **159,** 137–154.

Song, I., and Smith, W. L. (1996). C-terminal Ser/Pro-Thr-Glu-Leu tetrapeptides of prostaglandin endoperoxide H synthases-1 and -2 target the enzymes to the endoplasmic reticulum. *Arch. Biochem. Biophys.* **334,** 67–72.

Spriggs, M. K. (1996). One step ahead of the game: Viral immunomodulatory molecules. *Annu. Rev. Immunol.* **14,** 101–131.

Turner, P. C., and Moyer, R. W. (1998). The control of apoptosis by poxviruses. *Semin. Virol.* **8,** 453–469.

Upton, C., DeLange, A. M., and McFadden, G. (1987). Tumorigenic poxviruses: Genomic organization and DNA sequence of the telomeric region of the Shope fibroma virus genome. *Virology* **160,** 20–30.

Upton, C., Mossman, K., and McFadden, G. (1992). Encoding of a homolog of the interferon-γ receptor by myxoma virus. *Science* **258,** 1369–1372.

Verhoven, B., Schlegel, R. A., and Williamson, P. (1995). Mechanisms of phosphatidylserine exposure, a phagocyte recognition signal, on apoptotic T lymphocytes. *J. Exp. Med.* **182,** 15597–15601.